Cxcr2 and Cxcl5 regulate the IL-17/G-CSF axis and neutrophil homeostasis in mice

Junjie Mei,[1] Yuhong Liu,[1] Ning Dai,[1] Christian Hoffmann,[2,3] Kristin M. Hudock,[4]
Peggy Zhang,[1] Susan H. Guttentag,[1,5] Jay K. Kolls,[6] Paula M. Oliver,[7,8]
Frederic D. Bushman,[3] and G. Scott Worthen[1,5]

[1]Division of Neonatology, Children's Hospital of Philadelphia, Philadelphia, Pennsylvania, USA. [2]Instituto de Ciências Biológicas,
Universidade Federal de Goiás, Goiania, Brazil. [3]Department of Microbiology, [4]Department of Medicine, and [5]Department of Pediatrics,
Perelman School of Medicine, University of Pennsylvania, Philadelphia, Pennsylvania, USA.
[6]Richard King Mellon Foundation Institute for Pediatric Research, University of Pittsburgh School of Medicine, Pittsburgh, Pennsylvania, USA.
[7]Division of Cellular Pathology, Children's Hospital of Philadelphia, Philadelphia, Pennsylvania, USA.
[8]Department of Pathology and Laboratory Medicine, Perelman School of Medicine, University of Pennsylvania, Philadelphia, Pennsylvania, USA.

Neutrophils are essential for maintaining innate immune surveillance under normal conditions, but also represent a major contributor to tissue damage during inflammation. Neutrophil homeostasis is therefore tightly regulated. Cxcr2 plays a critical role in neutrophil homeostasis, as $Cxcr2^{-/-}$ mice demonstrate mild neutrophilia and severe neutrophil hyperplasia in the bone marrow. The mechanisms underlying these phenotypes, however, are unclear. We report here that Cxcr2 on murine neutrophils inhibits the IL-17A/G-CSF axis that regulates neutrophil homeostasis. Furthermore, enterocyte-derived Cxcl5 in the gut regulates IL-17/G-CSF levels and contributes to Cxcr2-dependent neutrophil homeostasis. Conversely, G-CSF was required for Cxcl5-dependent regulation of neutrophil homeostasis, and inhibition of IL-17A reduced plasma G-CSF concentrations and marrow neutrophil numbers in both $Cxcl5^{-/-}$ and $Cxcr2^{-/-}$ mice. $Cxcr2^{-/-}$ mice constitutively expressed IL-17A and showed increased numbers of IL-17A–producing cells in the lung, terminal ileum, and spleen. Most IL-17–producing splenocytes were responsive to IL-1β plus IL-23 in vitro. Depletion of commensal microbes by antibiotic treatment in $Cxcr2^{-/-}$ mice markedly decreased IL-17A and G-CSF expression, neutrophilia, and marrow myeloid hyperplasia. These data suggest a critical role for Cxcr2, Cxcl5, and commensal bacteria in regulation of the IL-17/G-CSF axis and neutrophil homeostasis at mucosal sites and have implications for the development of treatments for pathologies resulting from either excessive or ineffective neutrophil responses.

Introduction

Neutrophils are an essential component of innate immunity and host defense against bacterial and fungal infections by virtue of their rapid response to potential pathogens. In addition to this beneficial role, neutrophils are also a major contributor to tissue damage during inflammation (1). Under normal conditions, neutrophils are involved in immune surveillance for invading pathogens and exhibit extraordinary dynamics. As a short-lived cell (2), the disappearance of neutrophils from circulation must be balanced by BM production, and thus homeostasis is tightly controlled in the BM and circulation. In the BM, neutrophil numbers are tightly regulated through the balance between steady-state granulopoiesis and neutrophil release into the circulation. In adults the BM maintains a reservoir of neutrophils that can be mobilized into the circulation upon infection. Under basal conditions, only 1%–2% of total mature neutrophils in the body are in the circulation (3). While the mechanisms accounting for tight regulation of steady-state neutrophil homeostasis are not yet clear, neutrophil production is regulated on several levels by the potent granulocytic cytokine G-CSF. Furthermore, recent evidence indicates important roles for CXC chemokines containing the ELR motif (ELR+) and their only murine receptor, Cxcr2, balanced against the action of Cxcl12 (SDF-1) and its receptor, Cxcr4 (4, 5).

G-CSF stimulates the production and maturation of neutrophils by promoting the proliferation and differentiation of myeloid progenitors (6, 7) and has been widely used to treat or prevent neutropenia. In addition, G-CSF promotes neutrophil release from the BM into the circulation by either inducing expression of CXCR2 ligands or inhibiting the expression and signaling of SDF-1 and CXCR4 (4, 8–11). CXCL1 and CXCL2 mobilize neutrophils from the BM, and G-CSF may induce the expression of CXCR2 ligands involved in mobilization (4, 12).

Only recently has feedback control of G-CSF (Csf3) production been suggested. Stark et al. showed that the ingestion of apoptotic neutrophils by tissue phagocytes decreases G-CSF expression, thus limiting the stimuli for neutrophil production when neutrophils are available at (as yet unspecified) tissue sites (13). Using integrin β2–deficient mice and mice deficient in other adhesion molecules that exhibit defects in neutrophil emigration from blood into the tissues, Stark and colleagues suggested that the higher peripheral neutrophil numbers in blood are associated with increased IL-23 and IL-17 expression due to absence of an inhibitory signal associated with phagocytosis of apoptotic neutrophils (13). IL-23 stimulates IL-17 expression, which can be produced by αβ T cells, γδ T cells, NK cells, invariant NKT cells, and innate lymphoid cells (14, 15). The resultant high level of systemic G-CSF, and possibly other IL-17–stimulated cytokines such as GM-CSF and IL-6, contribute to exuberant neutrophil production and mobilization in the BM and high peripheral neutrophil numbers in $Itgb2^{-/-}$ mice. In contrast, it has been suggested that in normal mice, IL-23 and subsequent IL-17 production is attenuated upon neutrophil interaction with
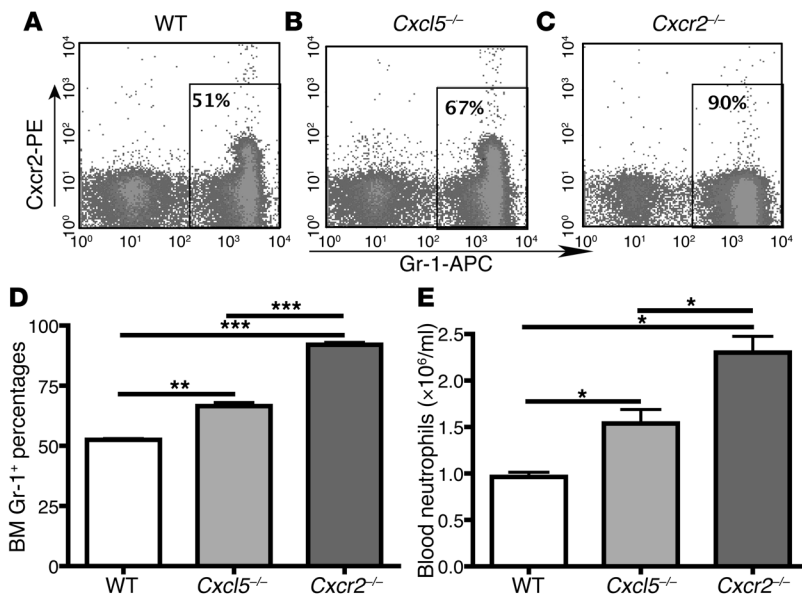
Figure 1
Cxcr2 inhibits neutrophil hyperplasia in BM and neutrophilia, and Cxcl5 plays a role in Cxcr2-regulated neutrophil homeostasis. (**A**–**C**) Representative histogram of flow cytometry histograms of BM cells from WT (**A**), *Cxcl5*⁻/⁻ (**B**), and *Cxcr2*⁻/⁻ (**C**) mice. After rbc lysis, BM cells were stained for Gr-1, and Cxcr2 expression was determined by flow cytometry. (**D**) The BM Gr-1⁺ cell percentages from WT, *Cxcl5*⁻/⁻, and *Cxcr2*⁻/⁻ mice (n = 5 mice/group) were analyzed by flow cytometry. (**E**) The blood neutrophil numbers from WT, *Cxcl5*⁻/⁻, and *Cxcr2*⁻/⁻ mice (n = 9 mice/group) was measured with a Hemavet 950 Automated Veterinary Analyzer. Data are representative of 2 independent experiments; values are means ± SEM. *$P < 0.05$; **$P < 0.01$; ***$P < 0.001$.

mononuclear phagocytes in the tissues, thereby limiting IL-17 and regulating basal G-CSF plasma level (13, 16). This feedback mechanism would thus regulate neutrophil production and mobilization and keep neutrophil homeostasis under tight control. However, we do not know whether induction of IL-17–producing cells and release of IL-17 and G-CSF is a constitutive process or is stimulated to some extent. In addition, the signals used to attract neutrophils to sites where they may influence expression of cytokines by tissue macrophages or dendritic cells remain unknown.

Cxcr2 has typically been described as a neutrophil chemokine receptor, although it is also expressed on other cell lineages such as endothelial cells (17, 18). In *Cxcr2*⁻/⁻ mice, immunity against bacterial infection is severely compromised due to the defective neutrophil chemotaxis (19, 20). Cxcr2 ligands belong to a family of ELR⁺ CXC chemokines that includes Cxcl1 (KC), Cxcl2 (Mip-2), Cxcl5 (Lix), and Cxcl15 (lungkine) in mice. Generally they are thought to be redundant, and Cxcr2 is currently considered to be their only functional receptor in mice. Recently we generated Cxcl5-deficient mice and uncovered a critical and unique role of Cxcl5 in regulating chemokine scavenging and pulmonary inflammatory responses (21).

The observation of neutrophilia and myeloid hyperplasia in mice lacking the chemokine receptor Cxcr2 was made many years ago (22, 23). Recently Eash et al. (4) showed that Cxcr2 deficiency produces a mouse model of myelokathexis syndrome with accumulation of mature neutrophils in the BM. They demonstrated that Cxcr2 antagonized Cxcr4-mediated neutrophil retention in the BM (4), as we had previously suggested (5). Their data indicated that G-CSF enhances expression of Cxcr2 ligands and inhibits SDF-1 expression in the BM, thus promoting neutrophil mobilization. In addition, their findings suggested that G-CSF–induced neutrophil release from the BM is Cxcr2 dependent. Despite these insights, the potential sources and mechanism of G-CSF expression in *Cxcr2*⁻/⁻ mice, and the contribution of G-CSF to the granulocyte hyperplasia characteristic of myelokathexis, remain unclear.

In this study we suggest what we believe is a novel mechanism that contributes to the myeloid hyperplasia phenotypes of *Cxcr2*⁻/⁻ mice in the BM. *Cxcr2*⁻/⁻ mice exhibited dramatically increased

circulating G-CSF and IL-17A (Il17a), in contrast to basal G-CSF levels and undetectable IL-17A levels in the blood of WT mice, thus indicating activation of IL-17A/G-CSF expression in *Cxcr2*⁻/⁻ mice. We demonstrate here that neutrophils expressing Cxcr2 were necessary for feedback inhibition of the IL-17A/G-CSF axis in tissues, particularly at mucosal sites. IL-1β/IL-23–responsive IL-17A–producing cells were significantly increased in tissues of *Cxcr2*⁻/⁻ mice relative to WT mice. Using *Cxcl5*⁻/⁻ mice, we found that resident cell–derived (but not hematopoietic cell–derived) Cxcl5 regulated neutrophil homeostasis under normal conditions, and both G-CSF and IL-17A signaling were essential for Cxcl5-regulated neutrophil homeostasis. Immunostaining showed that Cxcl5 was expressed under basal conditions in alveolar type II epithelial (AE II) cells in the lung and in enterocytes in the terminal ileum. Furthermore, inhibition of IL-17 and G-CSF expression in *Cxcr2*⁻/⁻ mice following antibiotic treatment suggested a model in which commensal bacteria help determine the set point for granulopoiesis through IL-17, G-CSF, and Cxcr2 ligands.

Results

Cxcr2 and Cxcl5 regulate neutrophil homeostasis in the BM and blood. We previously showed that *Cxcl5*⁻/⁻ mice (on a B6/129 mixed background) displayed a larger neutrophil population in the BM compared with WT mice (21). Since Cxcr2 deficiency leads to neutrophil hyperplasia in the BM and neutrophilia in the blood (4, 22, 23), we examined the effect of Cxcl5 and Cxcr2 in regulating BM neutrophil population and blood neutrophil number. Using *Cxcr2*⁻/⁻ and *Cxcl5*⁻/⁻ mice on a C57BL/6 background, we confirmed the dramatic myeloid hyperplasia phenotype of *Cxcr2*⁻/⁻ mice and found that Cxcl5 deficiency led to increased Gr-1⁺ cells in the BM and increased neutrophil counts in blood, which was an intermediate phenotype between WT and *Cxcr2*⁻/⁻ mice (Figure 1). As Cxcr2 is the sole functional receptor for ELR⁺ CXC chemokines (including Cxcl5) in mice, this suggests that Cxcl5 plays a role in Cxcr2-regulated neutrophil homeostasis in both BM and blood under normal conditions.

Neutrophil Cxcr2 regulates neutrophil homeostasis and the IL-17a/G-CSF axis. In order to determine whether the IL-17/G-CSF pathway was involved in stimulating granulopoiesis in the absence of Cxcr2, we measured
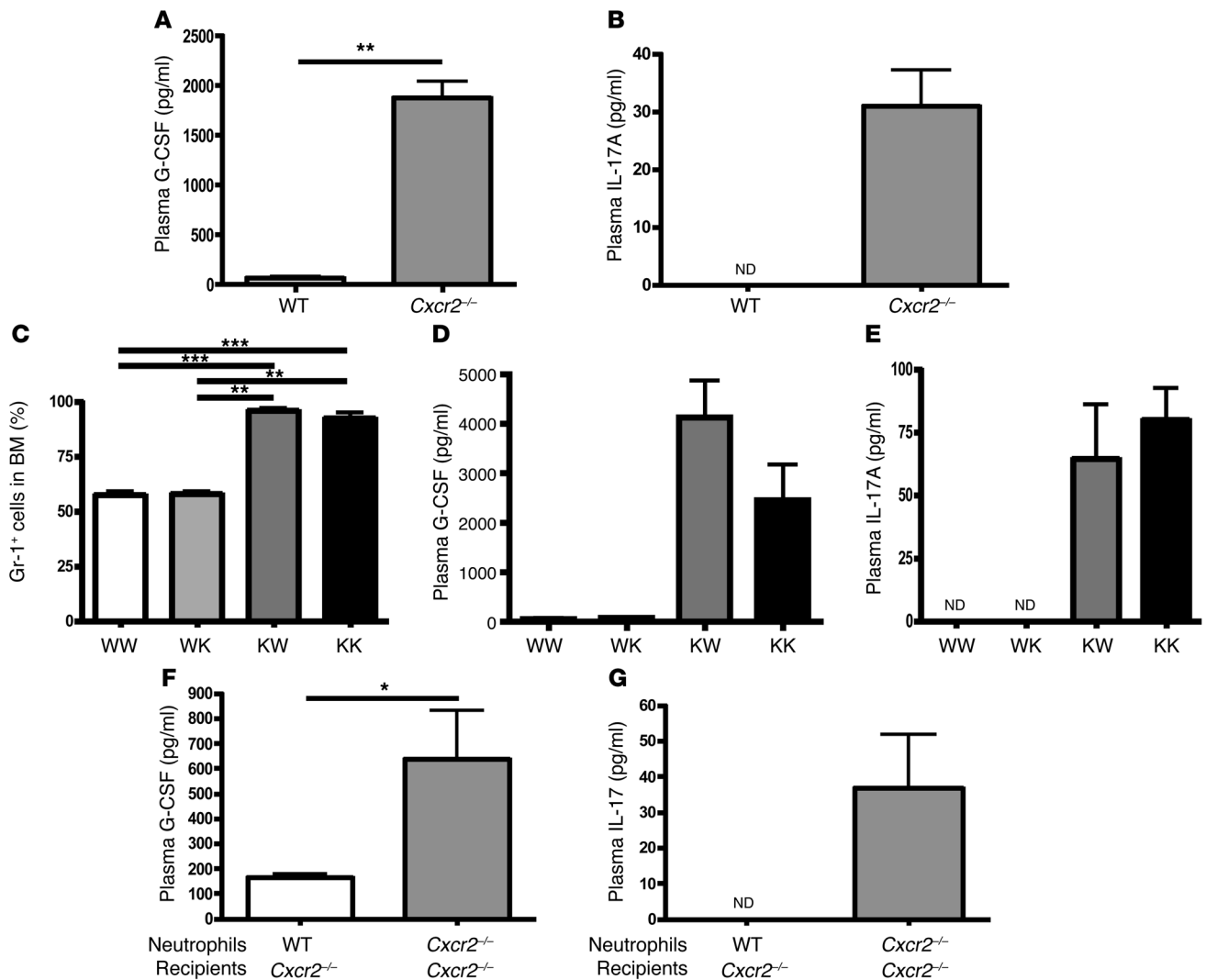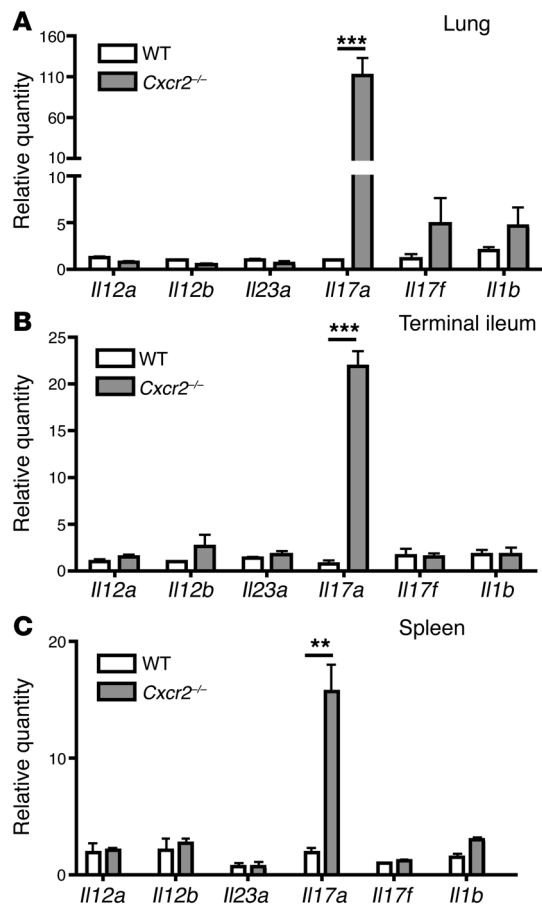
Figure 2
Cxcr2 on neutrophils inhibits G-CSF and IL-17A expression in plasma and regulates neutrophil homeostasis in the BM. (**A** and **B**) The plasma G-CSF (**A**) and IL-17A (**B**) levels in WT and *Cxcr2*^{−/−} mice (*n* = 4 mice/group) were measured by ELISA. (**C–E**) The Gr-1^{+} cell percentages (**C**) from the BM of the BM-reconstituted mice (*n* = 4 mice/group) were determined by flow cytometry, and the plasma levels of G-CSF (**D**) and IL-17A (**E**) were measured by ELISA. WW, WT BM into WT recipient mice; WK, WT BM into *Cxcr2*^{−/−} recipient mice; KW, *Cxcr2*^{−/−} BM into WT recipient mice; KK, *Cxcr2*^{−/−} BM into *Cxcr2*^{−/−} recipient mice. Isolated BM neutrophils (10[7]) from WT and *Cxcr2*^{−/−} mice were intravenously injected into *Cxcr2*^{−/−} mice (*n* = 3 mice/group). (**F** and **G**) After 24 hours, the plasma was prepared by coagulation-negative bleeding, and the plasma levels of G-CSF (**F**) and IL-17A (**G**) were measured by ELISA. ND, not detected. Values are means ± SEM. *$P < 0.05$; **$P < 0.01$; ***$P < 0.001$.

plasma levels of G-CSF and IL-17. In contrast to WT mice, in which G-CSF was nearly undetectable in the plasma (Figure 2A), the plasma concentrations of G-CSF were much higher in *Cxcr2*^{−/−} mice. IL-17A was detected at concentrations of approximately 40 pg/ml in *Cxcr2*^{−/−} mice, whereas it was undetectable in WT mice (Figure 2B). To determine which cells expressing Cxcr2 were involved in this process, we carried out BM reconstitution experiments using WT and *Cxcr2*^{−/−} mice. As seen in Figure 2, C–E, our data indicated that Cxcr2 deficiency confined to the hematopoietic lineage led to profound neutrophil hyperplasia in the BM (Figure 2C) and increased plasma levels of G-CSF (Figure 2D) and IL-17A (Figure 2E).

To further determine whether increased expression of G-CSF and IL-17 in hematopoietic Cxcr2 deficiency is specifically caused by absence of Cxcr2 on neutrophils, we adoptively transferred 1 × 10^{7}

purified WT or *Cxcr2*^{−/−} neutrophils (>90% neutrophils) into *Cxcr2*^{−/−} mice. After 24 hours, the mice injected with WT neutrophils showed significantly reduced plasma levels of G-CSF and IL-17A compared with those injected with *Cxcr2*^{−/−} neutrophils (Figure 2, F and G), indicating that neutrophil expression of Cxcr2 is sufficient to regulate G-CSF and IL-17A expression in the blood.

IL-17a expression is dramatically increased in the tissues of Cxcr2^{−/−} *mice.* We observed low but detectable levels of IL-17A in the blood of *Cxcr2*^{−/−} mice (Figure 2B). IL-23, which is a heterodimer consisting of IL-23a (p19) and IL-12b (p40), has been suggested to be the major amplifying signal for IL-17A production. Recently, it was suggested that IL-1β is crucial for the differentiation of IL-17–producing T cells and synergizes with IL-23 (24–26). To determine whether the expression of these genes is increased in the tissues of

Figure 3
Cxcr2 deficiency leads to dramatically increased IL-17A expression in the tissues. (**A–C**) Lung (**A**), terminal ileum (**B**), and spleen (**C**) from WT and *Cxcr2−/−* mice (*n* = 4 mice/group) were homogenized, and real-time PCR was performed using total RNA to determine the relative mRNA expression of *Il17a*, *Il17f*, *Il23a*, *Il12b*, *Il12a*, and *Il1b* in comparison with 18S rRNA. Values are means ± SEM. **$P < 0.01$; ***$P < 0.001$.

Cxcr2−/− mice, we measured the mRNA expression of *Il23a*, *Il12b*, *Il12a*, *Il17a*, *Il17f*, and *Il1b* in the lung (Figure 3A), terminal ileum (Figure 3B), and spleen (Figure 3C) of WT and *Cxcr2−/−* mice. Only *Il17a* mRNA levels were dramatically elevated in these tissues of *Cxcr2−/−* mice relative to WT mice, indicating that Cxcr2 limits IL-17A expression in these tissues.

Resident cell–derived Cxcl5 is responsible for regulating neutrophil homeostasis in the BM, and AE II cells and enterocytes express Cxcl5 under normal conditions. We previously demonstrated that under normal conditions, Cxcl5 in blood is derived from platelets (21), whereas in mouse models of lung inflammation, resident cells (which we have suggested are AE II cells; refs. 21, 27) are the only source of Cxcl5 in the bronchoalveolar lavage fluid (BALF). To determine the origin of the Cxcl5 contributing to neutrophil homeostasis, we generated BM chimeric mice using WT and *Cxcl5−/−* mice and found that only *Cxcl5−/−* recipient mice displayed increased percentages of neutrophil in the BM (Figure 4A), indicating that resident cell–derived Cxcl5 is responsible for regulating neutrophil homeostasis. This result is surprising, since under basal conditions the plasma Cxcl5 is derived from platelets but not from resident cells

(21), indicating that plasma Cxcl5 in normal WT mice does not contribute to neutrophil homeostasis. Taken together these data suggest that resident cell–derived Cxcl5 interacts with neutrophil Cxcr2 to regulate neutrophil homeostasis.

We previously showed that lung resident cells are the predominant source of Cxcl5 in the alveolar space during lung inflammation (21, 27). To further determine whether lung epithelial cells express measurable Cxcl5 under basal conditions, we used a small-volume lavage procedure to minimize dilution, and we detected low-level Cxcl5 expression (Figure 4B). BM reconstitution further showed that only lung resident cells were the source of homeostatic Cxcl5 in the lung (Figure 4C). In addition, isolated mouse lung epithelial cells cultured in the presence or absence of brefeldin A for 4 hours expressed and secreted the precursor (the less-active Lix93) and active form of Cxcl5 (Lix70). Furthermore, brefeldin A blocked the secretion of Cxcl5 into the medium and the maturation of Lix93 precursor into active Lix70 (Figure 4D). We also detected low-level Cxcl5 in the homogenates of the terminal ileum of WT mice (data not shown). To further determine whether gut resident cells express Cxcl5 under basal conditions, and to avoid the contamination of abundant Cxcl5 from platelets, we generated BM chimeric mice and demonstrated the absence of large amounts of Cxcl5 in the serum of mice (derived from platelet coagulation) reconstituted with *Cxcl5−/−* BM (Figure 4E), which confirmed depletion. After saline perfusion of the gut to further deplete blood cells, only homogenates of ileum from WT recipient mice showed detectable Cxcl5 (Figure 4F), indicating that gut resident cells express Cxcl5 under basal conditions as well. Immunostaining of lung and terminal ileum samples 6 hours after intravenous injection of brefeldin A demonstrated that Cxcl5 colocalized with the AE II cell–specific marker ABCA3 (Figure 4G) and revealed Cxcl5 expression in enterocytes in the villi of terminal ileum (Figure 4H). These data demonstrate that lung AE II cells and gut enterocytes express Cxcl5 constitutively under normal conditions and suggest that mucosal regions in contact with the environment may express Cxcl5.

Cxcl5 deficiency increases Il17 mRNA expression in the gut, but not in the lung. Since deletion of Cxcr2 induced the expression of IL-17A and G-CSF in both blood and tissues (Figure 2) and Cxcl5 is one of the few known ligands of Cxcr2, we wished to determine whether *Cxcl5−/−* mice displayed altered IL-17A and G-CSF expression. As shown in Figure 5A, *Cxcl5−/−* mice exhibited higher plasma levels of G-CSF than those of WT mice, albeit much lower than those in *Cxcr2−/−* mice (Figure 2A). In contrast, IL-17A protein was not detected in the plasma of either WT or *Cxcl5−/−* mice (data not shown). In order to quantify expression with better sensitivity, we examined mRNA levels of *Il23a*, *Il12a*, *Il12b*, *Il1b*, *Il17a*, and *Il17f* in the lung (Figure 5B), terminal ileum (Figure 5C), and spleen (Figure 5D) of WT and *Cxcl5−/−* mice. The mRNA expression of *Il17a* and *Il17f* mRNA expression was only increased in the gut of *Cxcl5−/−* mice relative to that of WT mice, but in the lungs or spleens we detected no increase in *Il17a*, *Il17f*, *Il1b*, *Il12*, or *Il23*. These data suggest that gut (but not lung) resident cell–derived Cxcl5 contributes to the regulation of IL-17 and G-CSF expression as well as neutrophil homeostasis under basal conditions.

Characterization of IL-17a–producing cells. To further determine the mechanisms by which the deficiency of Cxcr2 and Cxcl5 leads to increased IL-17A production in different tissues, we characterized the IL-17A–producing cells in the lung, lamina propria (LP) of terminal ileum, and spleen. As seen in Figure 6, *Cxcr2−/−* mice showed increased proportions of IL-17A–producing cells in all 3 tissues relative to WT mice, whereas in *Cxcl5−/−* mice, the proportion of IL-17A–
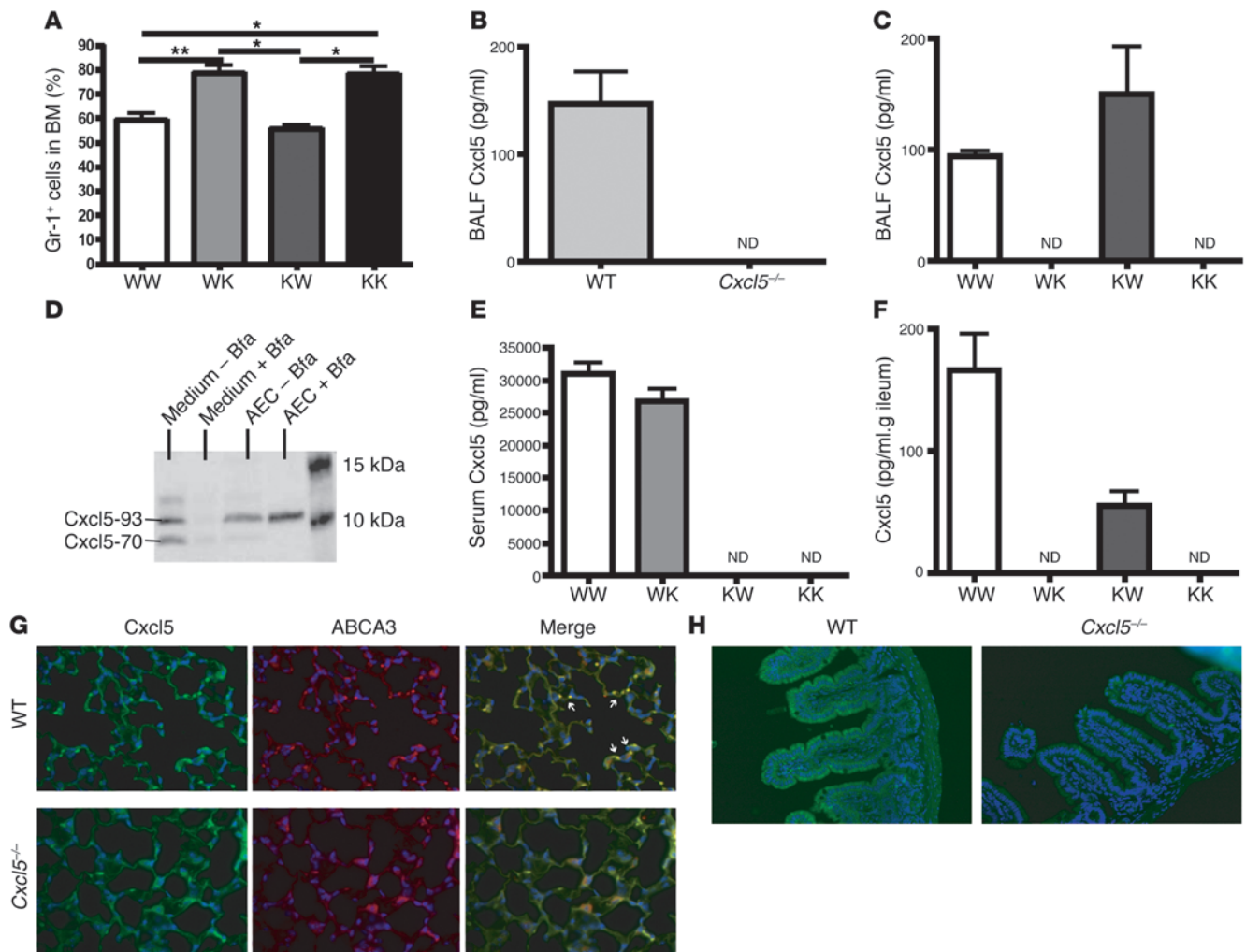
Figure 4
Resident cell–derived Cxcl5 is responsible for regulating neutrophil homeostasis in BM, and Cxcl5 is expressed by AE II cells in the lung and enterocytes in the ileum under basal conditions. (**A**) BM Gr-1^{+} cell percentages from BM-reconstituted mice ($n = 4$ mice/group) were determined by flow cytometry. WK, WT BM into $Cxcl5^{-/-}$ recipient mice; KW, $Cxcl5^{-/-}$ BM into WT recipient mice; KK, $Cxcl5^{-/-}$ BM into $Cxcl5^{-/-}$ recipient mice. (**B** and **C**) BALF (0.8 ml) was prepared from (**B**) naive WT and $Cxcl5^{-/-}$ mice ($n = 3$ mice/group) and (**C**) BM-reconstituted mice. Cxcl5 concentrations were measured by ELISA. (**D**) Lung epithelial cells were isolated from C57BL/6 mice and cultured for 24–48 hours with or without brefeldin A (added 4 hours before harvesting) and the medium and cell lysate immunoblotted for Cxcl5 expression. AEC, alveolar epithelial cell; Bfa, brefeldin A; M, molecular weight marker. (**E** and **F**) Serum concentrations of Cxcl5 (**E**) from BM chimeric mice ($n = 3$ mice/group) were measured by ELISA and the terminal ileum weighted, perfused, and homogenized in 1.4 ml saline, then Cxcl5 concentrations (**F**) were measured by ELISA. WT and $Cxcl5^{-/-}$ mice were intravenously injected with 0.25 mg brefeldin A. After 6 hours, lung and terminal ileum were perfused and fixed with formalin. (**G**) Lung samples immunostained for Cxcl5 and ABCA3. (**H**) Ileum samples immunostained for Cxcl5. White arrows indicate AE II cells. Original magnification, ×20. Values are means ± SEM. *$P < 0.05$; **$P < 0.01$.

producing cells only increased in the LP of terminal ileum, not in the lung or spleen (Figure 6 and Supplemental Figures 1–3; supplemental material available online with this article; doi:10.1172/JCI60588DS1), consistent with the *Il17a* mRNA expression patterns in these tissues (Figure 5). Among the IL-17A–producing cells in $Cxcr2^{-/-}$ mice, there were more CD3^{−} innate immune cells (including Gr-1^{+} cells, but not NK1.1^{+} NK cells) in the LP than in the lung and spleen (Figure 6 and Supplemental Figures 1 and 3); conversely, the CD3^{+} IL-17A–producing cells consisted mostly of αβ T cells and γδ T cells (Figure 6 and Supplemental Figures 1 and 2). In contrast to those in the lung and LP, most of the IL-17A–producing cells in the spleen of $Cxcr2^{-/-}$ mice were CD3^{+} T cells.

Since quantification of IL-17A–producing cells by flow cytometry is typically performed by ex vivo stimulation with non-physiologic agents, we wished to determine whether physiologic cytokines regulate these cells as well. It was recently reported that IL-1 signaling coordinates with IL-23 to promote the differentiation of IL-17A–producing T cells (25, 26), and so we tested in vitro stimulation using this combination. As seen in Figure 7, treatment of splenocytes of $Cxcr2^{-/-}$ mice with IL-1β plus IL-23 increased the percentages of IL-17A–producing cells (only slightly less than phorbol myristate acetate [PMA] plus calcium ionophore stimulation) (Figure 7), while none of these stimuli increased the numbers of IL-17A–producing cells in the splenocytes of WT or
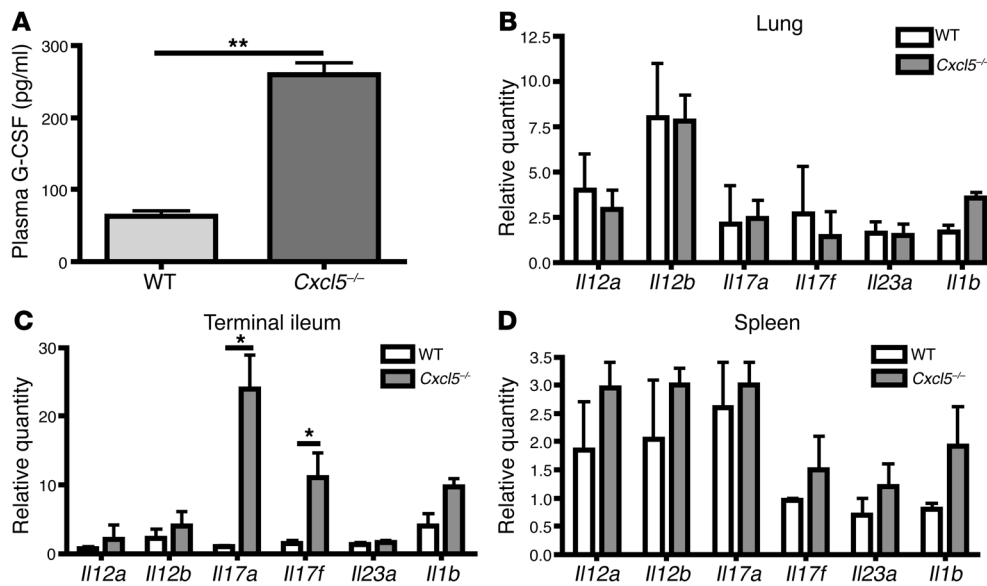
Figure 5
Cxcl5 decreases plasma G-CSF expression and *Il17a* mRNA expression in the gut, but not in the lung or spleen. (**A**) Plasma G-CSF from WT and *Cxcl5*−/− mice (*n* = 3 mice/group) was measured by ELISA. (**B**–**D**) Lung (**B**), terminal ileum (**C**), and spleen (**D**) from WT and *Cxcl5*−/− mice (*n* = 3 mice/group) were homogenized and real-time PCR performed from total RNA to determine the mRNA expression of *Il17a*, *Il17f*, *Il23a*, *Il12b*, *Il12a*, and *Il1b* relative to 18S rRNA. Values are means ± SEM. *$P < 0.05$; **$P < 0.01$.

Cxcl5−/− mice (data not shown). Neither IL-1β nor IL-23 stimulation alone increased the numbers of IL-17A–producing cells in the splenocytes of *Cxcr2*−/− mice (Figure 7). These data suggest that most IL-17A–producing splenocytes in *Cxcr2*−/− mice respond to IL-1β/IL-23 signaling, and thus IL-1β and IL-23 signaling may be involved in the constitutive expression of IL-17A in *Cxcr2*−/− mice.

The IL-17/G-CSF axis is essential for Cxcl5- and Cxcr2-regulated neutrophil homeostasis. Having implicated both G-CSF and IL-17A in granulocyte hyperplasia, we wished to determine the extent to which Cxcl5-regulated neutrophil homeostasis depends on this IL-17/G-CSF pathway. We generated *Cxcl5*−/−*Gcsf*−/− double-KO mice and found that both *Cxcl5*−/−*Gcsf*−/− and *Gcsf*−/− mice showed comparably reduced neutrophil population in the BM compared with WT and *Cxcl5*−/− mice (Figure 8A), indicating that Cxcl5-regulated neutrophil homeostasis is completely dependent on G-CSF. As for the role of IL-17A, inhibition of IL-17A signaling through treatment of anti–IL-17A antibodies in *Cxcl5*−/− (Figure 8, B and C) and *Cxcr2*−/− (Figure 8, D and E) mice significantly reduced the plasma G-CSF concentrations and BM neutrophil percentages compared with those treated with control IgG antibodies, indicating that IL-17A is essential for full expression of plasma G-CSF expression and neutrophil homeostasis in *Cxcl5*−/− and *Cxcr2*−/− mice. These data demonstrate the pivotal role of IL-17/G-CSF axis in Cxcl5- and Cxcr2-regulated neutrophil homeostasis in vivo. In addition, *Il17ra*−/− mice were found to have decreased neutrophil percentages in the BM (Supplemental Figure 4A) and undetectable plasma G-CSF (Supplemental Figure 4B) compared with WT mice, indicative of a critical of role of IL-17 signaling in G-CSF expression and hence neutrophil homeostasis.

Depletion of normal commensal bacteria leads to attenuation of the IL-17a/G-CSF axis and altered colonic bacterial community structure in WT and Cxcr2−/− *mice.* It was previously shown that germ-free *Cxcr2*−/− mice exhibited normal neutrophil counts in blood, while *Cxcr2*−/− mice under specific pathogen–free (SPF) conditions displayed blood neutrophilia (23). It is, however, unknown whether the neutrophil population in the BM of germ-free *Cxcr2*−/− mice is within the normal range. Therefore we hypothesized that commensal bacteria in mice may be necessary for activating the IL-17A/G-CSF axis, thus regulating neutrophil homeostasis in both BM and blood. To test

this hypothesis, we treated WT and *Cxcr2*−/− mice with antibiotics for 1 week to deplete the commensal bacteria. As shown in Figure 9A, antibiotic treatment decreased the commensal bacteria in the cecal samples by 4 logs in WT and *Cxcr2*−/− mice, as detected by 16S ribosomal DNA (rDNA) real-time PCR. Antibiotic treatment decreased BM neutrophil percentages, blood neutrophils, and plasma concentrations of IL-17A and G-CSF in *Cxcr2*−/− mice compared with untreated *Cxcr2*−/− mice (Figure 9, B–E). Even in WT mice, the basal-level plasma G-CSF became undetectable after antibiotic treatment. These data suggest that commensal microbes stimulate the IL-17A/G-CSF axis to upregulate BM granulopoiesis in *Cxcr2*−/− mice, and perhaps (albeit to a lesser extent) in normal mice.

In order to determine whether our antibiotic protocol altered gut community structure in a specific fashion, we analyzed microbial contents of cecum of WT and *Cxcr2*−/− mice with and without antibiotics using 454 sequencing of 16S rDNA. As seen in Figure 9F, the normal commensal flora of *Cxcr2*−/− mice is similar in broad outlines to that demonstrated for normal mice in other studies, being dominated by *Firmicutes* and *Bacteroidetes*. Following 7-day administration of antibiotics, as previously reported by Hill et al. (28), the community structure was clearly different ($P < 0.03$). Similar results were observed in WT mice between untreated and antibiotic-treated group (Supplemental Figure 5). In order to compare communities, we used both presence/absence information as well as the relative abundance data using unweighted and weighted Unifrac analysis, respectively, followed by principal coordinate analysis, as indicated in Supplemental Figures 6 and 7. Using these methods, all 4 groups were clearly identified within the first 3 coordinates, accounting for 45% and 86% of the variation present (unweighted and weighted Unifrac analysis, respectively). A global comparison of community structure confirmed large differences in the presence and absence of antibiotic treatment (Supplemental Figures 6 and 7). Analysis also suggested possible differences between WT and *Cxcr2*−/− mice in the absence of antibiotics, although differences among litters are also known to strongly influence microbiome composition, so a larger study is needed to distinguish possible genotypic differences from differences among litters and genders.
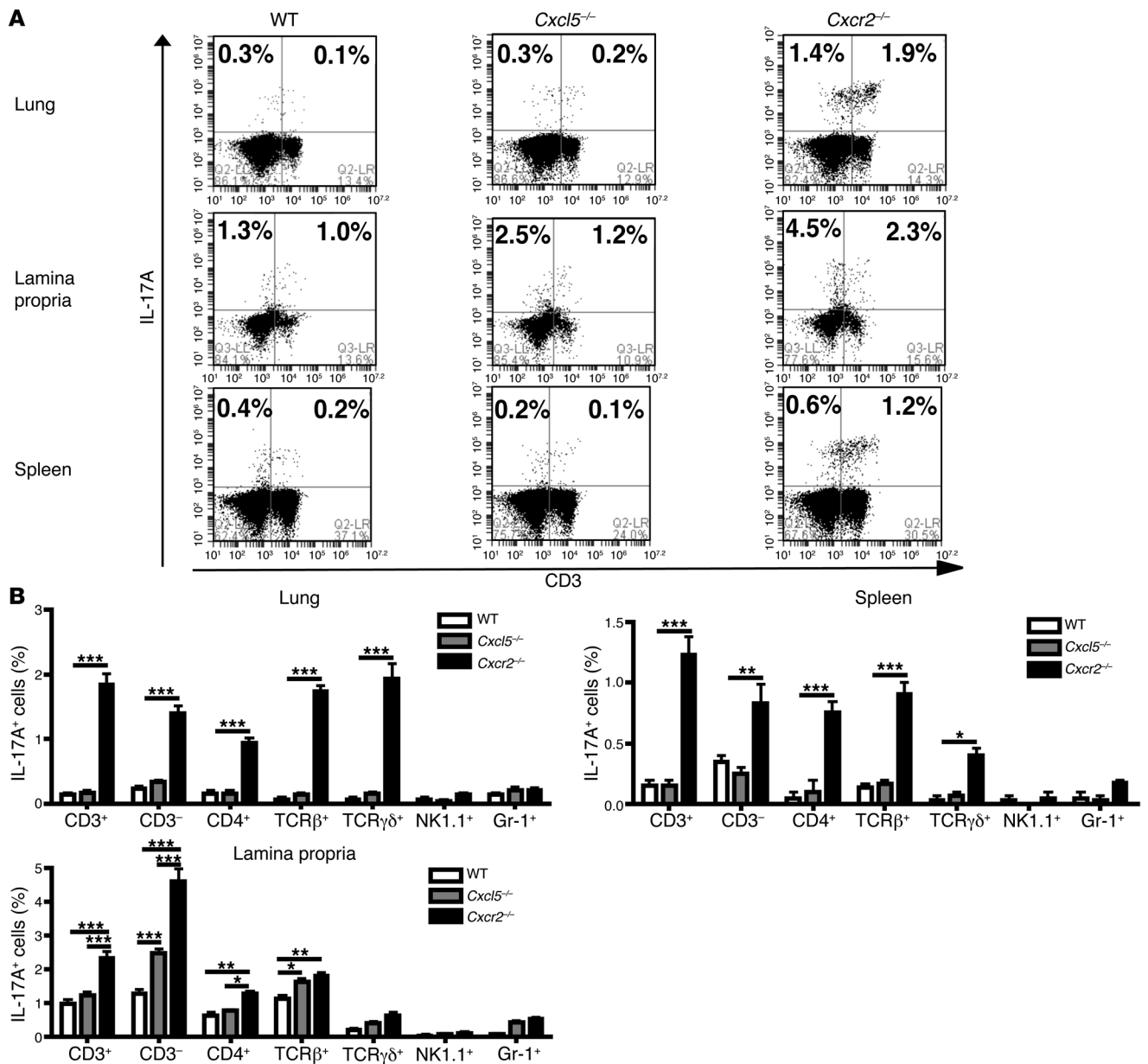
Figure 6

Characterization of IL-17A–producing cells in the lung, gut, and spleen of WT, *Cxcl5*⁻/⁻, and *Cxcr2*⁻/⁻ mice. (**A**) Representative flow cytometry histograms of isolated lung cells, LP cells from terminal ileum, and splenocytes from WT, *Cxcl5*⁻/⁻, and *Cxcr2*⁻/⁻ mice (*n* = 3 mice/group). These cells were immunostained for intracellular IL-17A and surface CD3 expression. Representative histograms with immunostaining for surface CD4, TCRβ, TCRγδ, Gr-1, NK1.1 and intracellular IL-17A are shown in Supplemental Figures 1–3. These histograms are the representative of 2 separate experiments with similar results. (**B**) IL-17A–producing cell percentages of different cell populations in the lung, LP of terminal ileum, and spleen. Values are means ± SEM. *P < 0.05; **P < 0.01; ***P < 0.001.

Discussion

Neutrophil homeostasis represents a delicately regulated balance among a series of processes, including granulopoiesis in the BM, neutrophil release into blood, neutrophil migration from the blood into tissues, and neutrophil apoptosis and clearance under both normal and inflammatory states. Tight control of neutrophils under normal and inflammatory conditions is a critical component of innate immunity. Hence, failure of neutrophil regulation may contribute to inflammatory diseases or worsening of infection. In contrast to the granulopoiesis that occurs in response to severe inflammatory stimuli, steady-state homeostasis employs mechanisms by which neutrophils are mobilized from BM to blood to maintain effective neutrophil number (which may reflect neutrophils in tissues as well as those in the circulation) despite routine stresses. Furthermore, neutrophil homeostasis may also include mechanisms by which neutrophil numbers rapidly decline upon resolution of inflammation in tissues and circulation (3, 29).
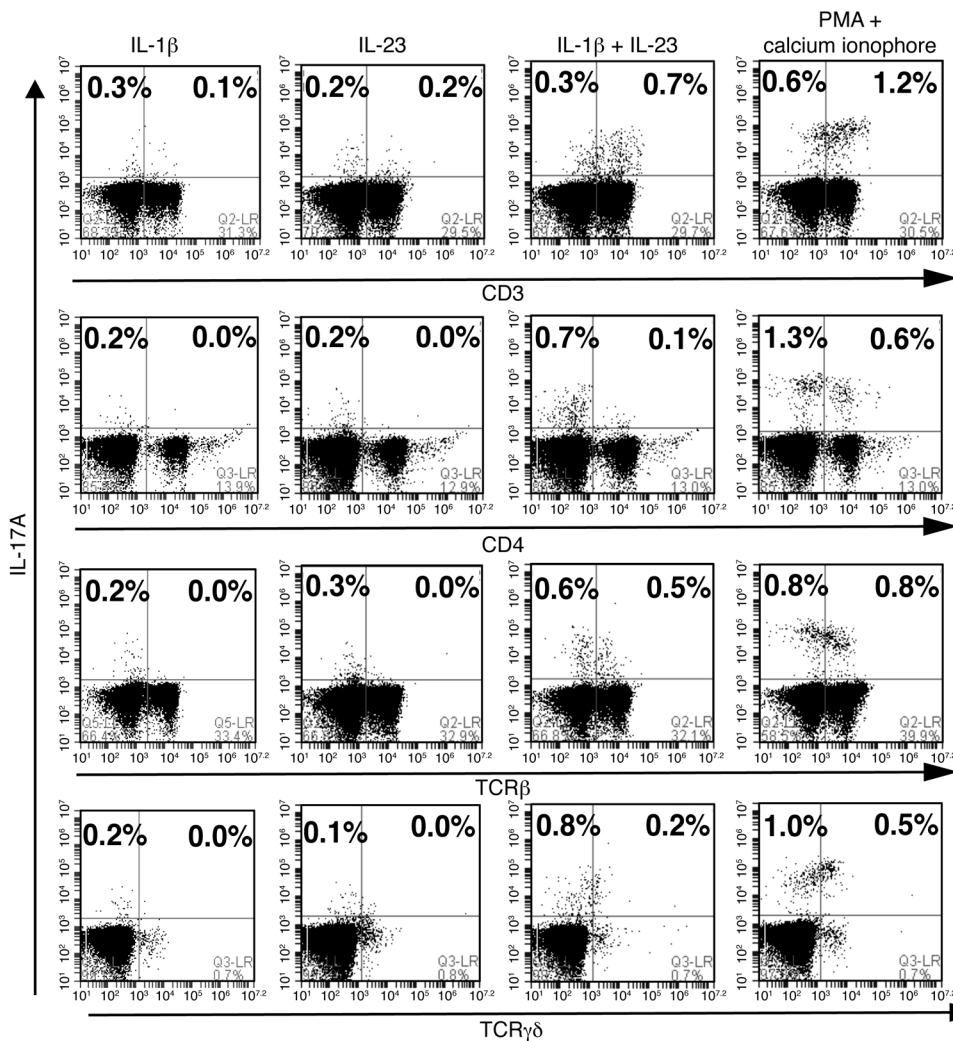
Figure 7
The synergistic effect of IL-1β and IL-23 on IL-17A production on the splenocytes of *Cxcr2*−/− mice. Representative flow cytometry histograms of isolated splenocytes from *Cxcr2*−/− mice in response to IL-1β, IL-23, IL-1β plus IL-23, and PMA plus calcium ionophore A23187 for 5 hours in the presence of Golgistop. Cells were immunostained for intracellular IL-17A and surface CD3, CD4, TCRβ, and TCRγδ expression. Histograms are representative of 2 separate experiments with similar results.

Recent advances in identifying the feedback control mechanisms regulating neutrophil production and release have indicated an important role for the IL-17/G-CSF pathway. In this study we uncover another layer in the regulation of neutrophil homeostasis via a feedback loop among Cxcr2, Cxcl5, and the IL-17/G-CSF axis. Specifically, we have demonstrated the critical role of neutrophil Cxcr2 and nonhematopoietic resident cell–derived Cxcl5 in regulating the IL-17/G-CSF axis and neutrophil homeostasis under basal conditions and, in turn, the essential role of this axis in Cxcl5-regulated neutrophil homeostasis. We propose a model in which Cxcr2, its ligands, and commensal bacteria control neutrophil homeostasis through the IL-17/G-CSF axis, primarily at mucosal sites (Figure 10). Based on our findings, we propose that at mucosal sites such as gut and lung, resident cells secrete Cxcr2 ligands to attract neutrophils into tissues to inhibit the IL-17/G-CSF axis, thus regulating neutrophil homeostasis under normal conditions. In this feedback loop, enterocyte-derived Cxcl5 in the gut, but not AE II cell–derived Cxcl5 in the lung, is required for inhibition of IL-17 production, while other Cxcr2 ligands may be responsible for Cxcr2-mediated regulation of IL-17/G-CSF axis in the lung. In addition, commensal bacteria are required for the activation of IL-17/G-CSF axis caused by Cxcr2 deficiency, and IL-1 and IL-23 signaling may serve to induce IL-17 production in vivo.

Granulopoiesis in the BM is an essential first step in neutrophil homeostasis. While we found extremely large numbers and percentages of neutrophils in the BM of *Cxcr2*−/− mice, this represents the net result of both enhanced granulopoiesis, as we show here, and release into the circulation. Link and colleagues showed that neutrophil Cxcr2 is required for G-CSF–mediated neutrophil mobilization from the BM to the blood (4). Therefore the high neutrophil percentages (about 90%) in the BM of *Cxcr2*−/− mice are due not only to G-CSF–induced granulopoiesis, but also to the additive effect of defective G-CSF–mediated neutrophil mobilization to the blood. The defect in release also contributes to a delay in the reduction of BM neutrophil percentages upon anti–IL-17A antibody treatment in *Cxcr2*−/− mice compared with that in *Cxcl5*−/− mice, despite the dramatically reduced plasma G-CSF in *Cxcr2*−/− mice (Figure 8, B–E). Furthermore, the defective neutrophil release in *Cxcr2*−/− mice also reduces the neutrophil numbers in the blood, which may explain the mild neutrophilia (a 2- to 4-fold increase relative to WT mice) observed in *Cxcr2*−/− mice, which is in contrast to the severe neutrophilia (about 20-fold increase relative to WT mice) observed in *Itgb2*−/− mice, despite the overwhelmingly dominant neutrophil population in the BM of *Cxcr2*−/− mice.

Based on the findings of Stark et al. (13), a critical step in neutrophil homeostasis is neutrophil migration to sites of interest. Our data suggest the critical role of neutrophil Cxcr2 and nonhema-
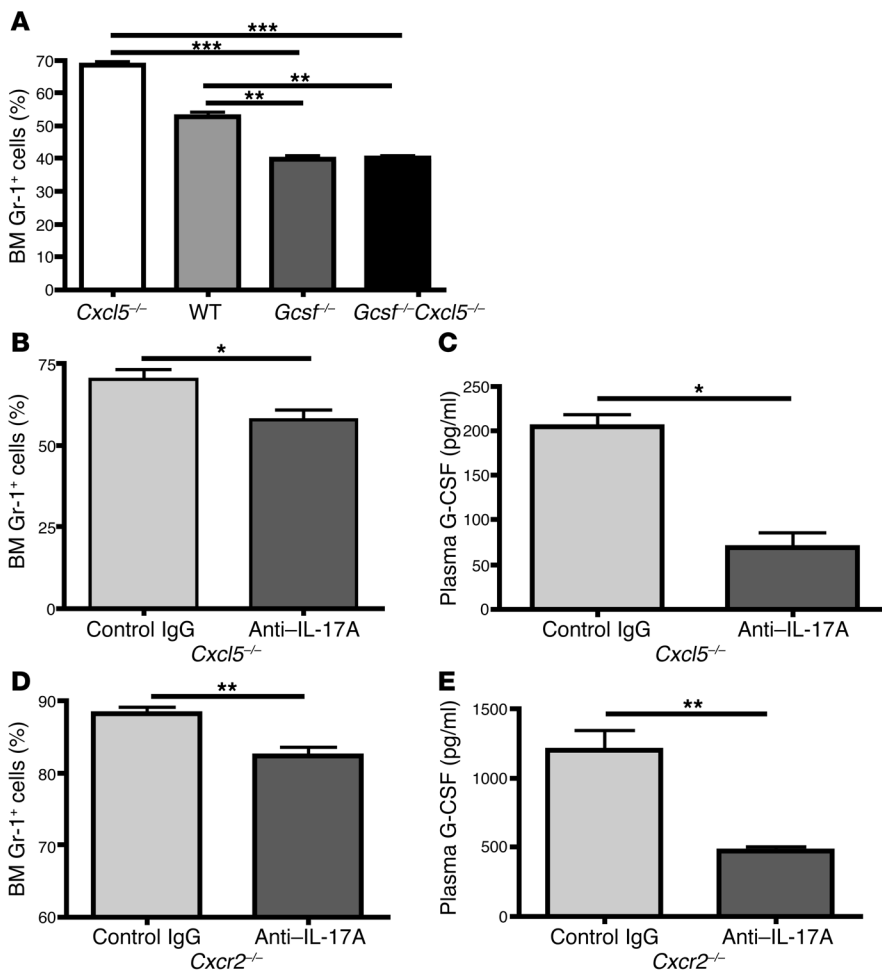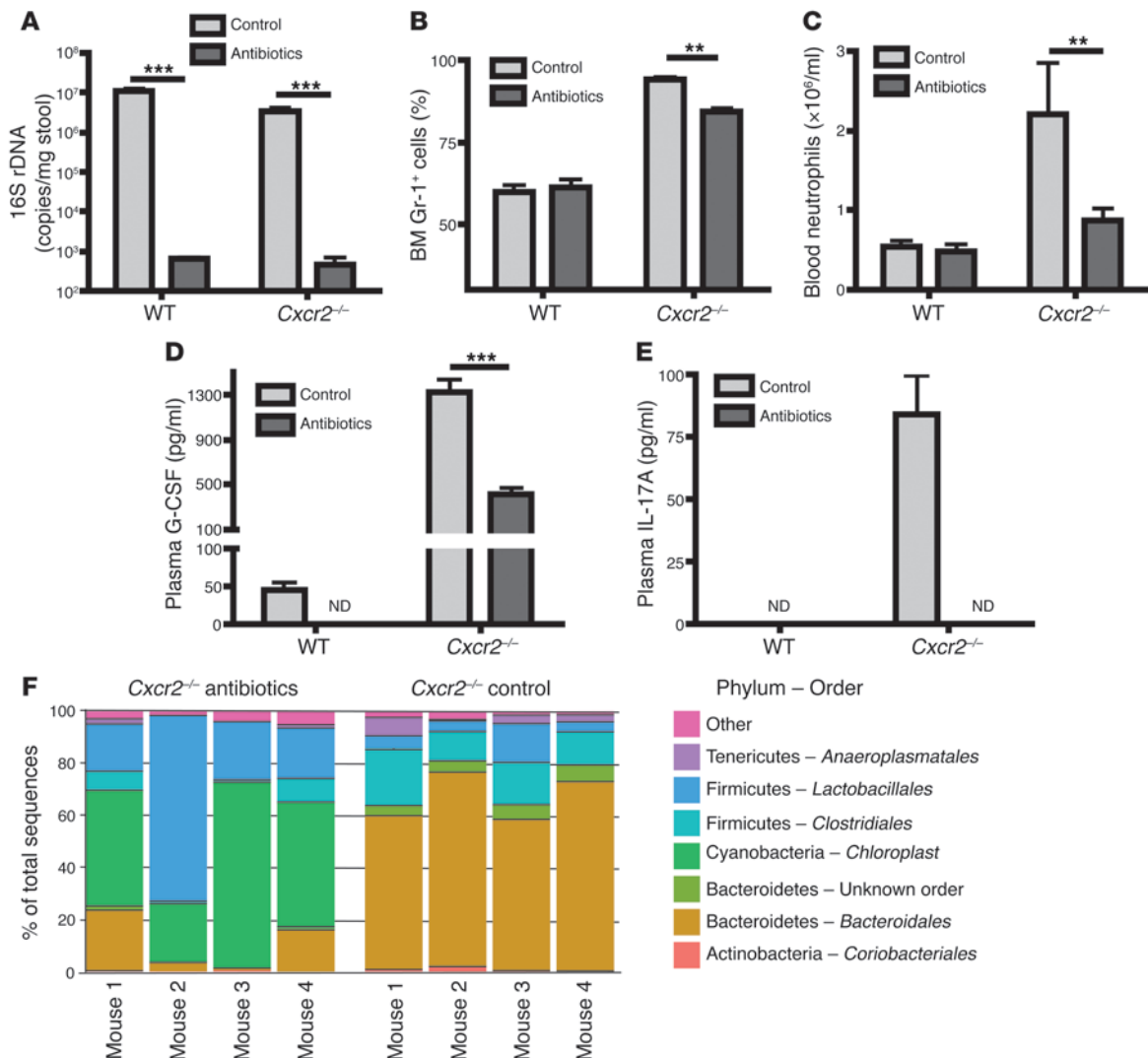
Figure 8
IL-17A/G-CSF axis is critical for Cxcl5- and Cxcr2-regulated neutrophil homeostasis. (**A**) BM Gr-1$^+$ cell percentages from WT, $Cxcl5^{-/-}$, $Gcsf^{-/-}$, and $Cxcl5^{-/-}Gcsf^{-/-}$ mice (n = 4 mice/group) were determined by flow cytometry. (**B**–**E**) $Cxcl5^{-/-}$ (**B** and **C**) and $Cxcr2^{-/-}$ (**D** and **E**) mice were treated with control IgG and anti–IL-17A antibodies 3 times over a 7-day period (n = 3 mice/group), the BM Gr-1$^+$ cell percentages (**B** and **D**) and plasma G-CSF concentrations (**C** and **E**) were determined using flow cytometry and ELISA, respectively. Values are means ± SEM. *P < 0.05; **P < 0.01; ***P < 0.001.

topoietic resident cell–derived Cxcr2 ligands such as Cxcl5 in this process. We propose that resident cells in the gut and lung express Cxcr2 ligands that attract neutrophils to migrate into the tissues, where they regulate the IL-17/G-CSF axis and neutrophil homeostasis. The dramatic increase in IL-17A/G-CSF and BM neutrophil percentages in the absence of Cxcr2 or Cxcl5 is the evidence of interruption of this feedback loop. In addition, we found that enterocytes in the ileum express Cxcl5 under basal conditions, consistent with a previous report that Cxcl5 was expressed in colonic enterocytes in a murine colitis model (30), suggesting that enterocyte-derived Cxcl5 mediates neutrophil transmigration into the gut to regulate steady-state neutrophil homeostasis.

While basal granulopoiesis is not thought to be responsive to the environment, we have shown here that the commensal bacteria of the gut serve a role in the regulation of the IL-17/G-CSF axis. It has been demonstrated that commensal bacteria are important for shaping intestinal immune responses under normal and inflammatory states (31). Segmented filamentous bacteria were recently identified to promote Th17 cell differentiation (32, 33); however, how commensal bacteria affect IL-17–producing cell differentiation and IL-17 production under normal and inflammatory conditions remains poorly understood. Here we showed that depletion of commensal bacteria through antibiotic treatment significantly decreased systemic IL-17/G-CSF expression, BM neutrophil percentages, and peripheral neutrophilia in $Cxcr2^{-/-}$ mice (Figure 9), which is consistent with previous

reports that germ-free $Cxcr2^{-/-}$ mice lost the neutrophilia phenotype observed in SPF $Cxcr2^{-/-}$ mice. These data suggest that commensal microbiota may contribute to signaling for IL-17 production in the gut, likely through pattern recognition receptors, thus regulating neutrophil homeostasis under normal conditions. WT mice administered antibiotics also exhibited decreased plasma baseline G-CSF (Figure 9). Cxcl5 deficiency led to increased IL-17–producing cells in the terminal ileum, but not in the lung, providing novel insights that different mucosal sites might utilize different Cxcr2 ligands (secreted by resident epithelial cells) to attract neutrophils into the tissues to regulate IL-17/G-CSF axis and neutrophil homeostasis under normal conditions. However, the signals used to attract neutrophils to sites where they may influence IL-23 and IL-1β expression by tissue macrophages or dendritic cells, and which tissues are involved, remain unclear and warrant further investigation.

In contrast to the role of the terminal ileum in the induction of IL-17, we observed that Cxcl5 regulation of IL-17 does not extend to the distal lung. Consistent with our prior work (27, 34), we demonstrate here that lung AE II cells express Cxcl5 at baseline. In $Cxcl5^{-/-}$ mice, however, dysregulation of IL-17 occurred only in the gut and not in the lung. We suspect that the inability of lung-derived Cxcl5 to inhibit IL-17 production may result from the relative sterility of the alveolar space limiting the activation of IL-17A/G-CSF axis, but we cannot at this time rule out the possibility that an alveolar microbiome exists and modifies IL-17A expression. We previously

Figure 9
Commensal bacteria promote IL-17A and G-CSF expression, neutrophilia, and BM neutrophil hyperplasia and alter colonic bacterial community structure in *Cxcr2^-/-* mice. WT and *Cxcr2^-/-* mice (n = 4–5 mice/group) were treated with or without antibiotics for 7 days. (**A**) 16S rDNA copy numbers from the cecal contents of WT and *Cxcr2^-/-* mice after treatment were determined using real-time PCR. (**B** and **C**) BM Gr-1^+ cell percentages (**B**) were determined using flow cytometry, and blood neutrophil numbers (**C**) were measured with a Hemavet 950 Automated Veterinary Analyzer. (**D** and **E**) Plasma G-CSF (**D**) and IL-17A (**E**) were measured using ELISA. (**F**) Phylum-order frequencies of cecal bacterial communities in *Cxcr2^-/-* mice treated with and without antibiotic treatment was determined using pyrosequencing of 16S rDNA. The gut microbial communities were significantly different between control mice and antibiotic-treated mice, regarding their composition as well as relative abundance as measured with unweighted and weighted Unifrac, respectively (unweighted Unifrac, $P \le 0.004$; weighted Unifrac, $P \le 0.026$). Values are means ± SEM. **$P < 0.01$, ***$P < 0.001$.

demonstrated high levels of another Cxcr2 ligand, lungkine (which is constitutively expressed by bronchial epithelial cells; ref. 35), in the BALF of normal mice (21). In addition, 2 other Cxcr2 ligands in mice, Cxcl1 and Cxcl2, can be induced by G-CSF (4, 36), implying that they may be involved in neutrophil release from BM. Whether Cxcl1 or Cxcl2 plays a role in regulating the IL-17/G-CSF axis and steady-state neutrophil homeostasis will require further investigation of their respective gene-targeted mice.

IL-17A–producing cells have been advanced as important controllers of inflammatory signaling (15, 37, 38). The explosion of data on the varied lineages of these cells indicates that many cells are candidates for production of IL-17A in our model. In contrast

to a recent study in a different model (13), we found that in our model, not only did Th17 and γδ T cells express IL-17A in lung, gut, and spleen, but cells that were not T cells from lung and gut were also able to generate IL-17. The identity of these cells remains unclear and is the subject of ongoing work. The signals responsible for IL-17–producing cells are somewhat better established, and IL-23 has emerged as an important mediator. In our model, we do not detect a significant increase for IL-23 expression in either *Cxcr2^-/-* or *Cxcl5^-/-* mice, perhaps because of detection limits or posttranscriptional regulation of this potent cytokine. However, our data highlight the potential importance of both IL-1 and IL-23 signaling in stimulation of IL-17–producing cells.
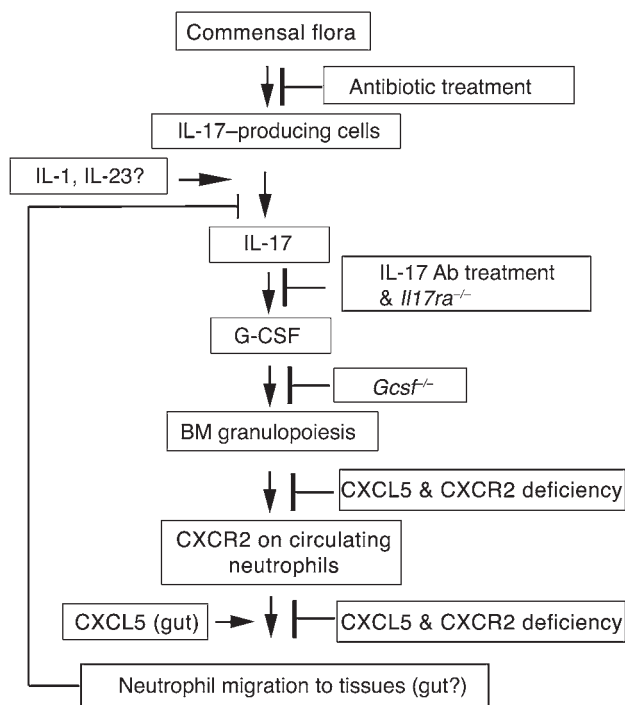
```
Commensal flora
      │
      ▼ ┤── Antibiotic treatment
IL-17–producing cells
      │
IL-1, IL-23? ──▶ │
      │           ▼
            IL-17
              │
              ▼ ┤── IL-17 Ab treatment
                   & Il17ra⁻/⁻
            G-CSF
              │
              ▼ ┤── Gcsf⁻/⁻
      BM granulopoiesis
              │
              ▼ ┤── CXCL5 & CXCR2 deficiency
      CXCR2 on circulating
         neutrophils
              │
CXCL5 (gut) ──▶ ▼ ┤── CXCL5 & CXCR2 deficiency
      Neutrophil migration to tissues (gut?)
```

Figure 10

The proposed roles of CXCR2, CXCL5, and commensal bacteria in neutrophil homeostasis under normal conditions. CXCR2 on neutrophils is required for neutrophil transmigration into tissues, especially at mucosal sites such as the gut and lung, to downregulate the IL-17/G-CSF axis and granulopoiesis. Gut enterocyte–derived CXCL5 attracts neutrophils through CXCR2 to transmigrate into the gut tissues to exert such regulatory effects on neutrophil homeostasis. In addition, CXCR2 on neutrophils is also required for G-CSF–mediated neutrophil release from BM to blood, although the CXCR2 ligands responsible for this process and the mechanisms remain unclear. Depletion of commensal bacteria by antibiotic treatment downregulates the IL-17/G-CSF axis and BM granulopoiesis in $Cxcr2^{-/-}$ mice, in which IL-1β and IL-23 signaling may be required for IL-17A production in the tissues.

Recently it has been shown that IL-1 signaling is crucial for IL-17 production and differentiation of early Th17 cells (25), IL-17–producing γδ T cells, and invariant NKT cells upon synergizing with IL-23 (24, 26). In these studies, the Th17 cells or IL-17–producing γδ T cells from spleens or lymph nodes significantly increased upon stimulation of IL-1β/IL-23 for 3 days. Here we stimulated splenocytes from WT, $Cxcl5^{-/-}$, and $Cxcr2^{-/-}$ mice for only 5 hours with IL-1β, IL-23, IL-1β/IL-23, and PMA/calcium (Figure 7). Only $Cxcr2^{-/-}$ mice had an increased percentage of IL-17A–producing cells (mostly CD3⁺ T cells) in response to IL-1β/IL-23 stimulation, albeit less than that upon stimulation of PMA/calcium ionophore, which suggests that combined signals may be required for optimal IL-17A expression.

In summary, we present a model in which Cxcr2, Cxcl5, and commensal bacteria regulate the IL-17/G-CSF axis and neutrophil homeostasis under basal conditions (see Figure 10 for a proposed scheme). This model predicts that the local environment, sensed at mucosal sites, contributes to setting the signals for neutrophil generation. It would be prudent to consider that the intensity of these baseline signals may also influence, through commensal bacteria, the organismal response to severe stress such as pneumonia or sepsis. This question will be the subject of further study.

Methods

Mice. All mice were kept in SPF conditions in the animal facility of the Children's Hospital of Philadelphia. $Cxcr2^{-/-}$, $Il17ra^{-/-}$, $Gcsf^{-/-}$, and WT control mice were on a C57BL/6J background. $Cxcl5^{-/-}$ mice were backcrossed with C57BL/6J mice for 6 generations and then bred with $Gcsf^{-/-}$ mice to generate $Cxcl5^{-/-}Gcsf^{-/-}$ mice. Sex- and age-matched 6- to 12-week-old mice were used for experiments.

Generation of chimeric mice by BM reconstitution. The generation of BM-reconstituted mice has been previously described (21). The 6- to 8-week-old recipient mice were lethally irradiated in 2 doses of 800 rad and 400 rad with an interval of 3 hours. The BM from donor mice was harvested from both tibiae and femora. After lysis of rbc, at least 5×10^6 cells were intravenously injected into recipient mice after lethal irradiation. The BM reconstitution was performed in 4 groups of mice: BM from WT mice into WT mice, BM from WT mice into KO mice, BM from KO mice into WT mice, and BM from KO mice into KO mice. 6–12 weeks after irradiation, the citrated blood and BM from 1 femur were harvested from chimeric mice.

FACS analysis. 1 femur from each mouse was separated and flushed with 5 ml 5% FCS DMEM medium. We then lysed rbc with ACK rbc lysis buffer. The remaining cells were counted and stained with propidium iodide (PI), PE-conjugated anti-Cxcr2 (R&D Systems), and APC-conjugated anti-Gr-1 antibody (BD Biosciences) and analyzed with a BD FACSCalibur flow cytometer.

Blood neutrophil count. Blood (50 μl) was collected into EDTA-coated tubes (Sarstedt Inc.) by retro-orbital bleeding, then the neutrophil numbers and percentages in the blood were determined using a Hemavet 950 Automated Veterinary Analyzer.

Western blot. The lysates of cultured alveolar epithelial cells and the concentrates of medium were fractionated on 18% Tris-glycine gels, then transferred on a polyvinylidene difluoride membrane using the standard protocols. The antibody to murine Cxcl5 (Peprotech) was used for detection.

Adoptive transfer of neutrophils. The BM of the femora and tibiae of WT and $Cxcr2^{-/-}$ mice were flushed with HBSS and layered on a 3-step Percoll (Pharmacia) gradient (72%, 64%, and 52%), which was centrifuged at $1,060 g$ for 30 minutes (5). The cell layer of the 72%:64% interface were collected and washed twice in PBS. Cytospin revealed that more than 95% of the isolated cells appeared to be morphologically mature neutrophils. Then, 1×10^7 isolated WT or $Cxcr2^{-/-}$ BM neutrophils were intravenously injected into $Cxcr2^{-/-}$ mice. After 24 hours, the murine citrated plasma samples were prepared as previously described (21) and the plasma G-CSF and IL-17A concentrations were measured by ELISA.

Inhibition of IL-17 signaling. Control isotype IgG or anti–IL-17A antibodies (100 μg; R&D Systems) were intraperitoneally injected into $Cxcl5^{-/-}$ mice at days 0, 3, and 6, and then the mice were sacrificed at day 7. The plasma G-CSF concentrations and BM Gr-1⁺ cell percentages were determined by ELISA and flow cytometry.

Isolation and immunostaining of tissue lymphocytes. Spleens were aseptically removed at the time of necropsy. Single-cell suspensions were obtained by gently pressing the spleen against a 100-μm strainer. For isolation of LP lymphocytes (39), freshly resected terminal ilea were washed with cold PBS and cut into 2- to 5-mm pieces, then incubated in HBSS solution containing 15 mM HEPES and 1 mM EDTA at room temperature 3 times, until debris and epithelial cells were removed and the supernatant solution appeared clear. Subsequently, tissues were digested in RPMI 1640 with 10% FBS, 15 mM HEPES, 1% penicillin/streptomycin, and 300 U/ml collagenase VIII (Sigma-Aldrich) at 37°C for 60 minutes. Then the lymphocytes were isolated at the 40%:80% interface of a discontinuous Percoll gradient.

Single cells isolated from lung, LP, and spleen were cultured in RPMI 1640 containing 10% FBS, 1× nonessential amino acids (Invitrogen), 10 mM HEPES, 2 mM L-glutamine, and 1% penicillin/streptomycin and Golgi-Stop (BD Biosciences — Pharmingen) for 5 hours with 10 ng/ml PMA

(Sigma-Aldrich) and 500 ng/ml calcium ionophore A23187 (Sigma-Aldrich). For cultured spleen cells, the stimulation was divided into 4 groups: recombinant IL-1β (R&D Systems; 10 μg/ml), IL-23 (R&D Systems; 10 μg/ml), IL-1β plus IL-23, and 10 ng/ml PMA plus 500 ng/ml calcium ionophore A23187.

The following antibodies were used for immunostaining: FITC-conjugated anti–β TCR, APC-conjugated anti–γδ TCR, FITC-conjugated anti-CD3, APC-conjugated anti-CD4, FITC-conjugated anti-NK1.1, and PE-conjugated anti–IL-17A antibodies (BioLegend Inc.) and APC-conjugated anti–Gr-1 antibody (BD Biosciences). After stimulation, cells were resuspended at 10^7 cells/ml. Fcγ II/III receptors were blocked with 0.5 μg anti-CD16/CD32, and the cell suspension was incubated with an optimal concentration of mAbs for 20 minutes at 4°C in staining buffer. Intracellular staining was performed using Fix and Perm cell permeabilization reagents (Caltag Laboratories). Flow cytometry was performed on an Accuri Flow Cytometer.

Culture of mouse lung epithelial cells. C57BL/6J mouse lungs were inflated in situ via tracheal cannulation with Dispase (approximately 0.7 ml, 50 U/ml), tied with a suture, transferred to a 50-ml conical tube, and incubated at room temperature for approximately 40 minutes. Lobes were dissected free and chopped mechanically, followed by incubation at 37°C for 10 minutes in MEM plus DNase I (20 μg/ml) to complete digestion. The mixed cells were filtered through a 100-μm cup filter, and fibroblasts were removed from the suspension by 3 successive adherence steps on plastic (approximately 40 minutes each). Negative selection was used to purify epithelial cells from macrophages and other blood cells using 2 magnetic bead kits (Dynabeads DC Cell Enrichment Kit, catalog no. 114.29D; Dynal Mouse T Cell Negative Isolation Kit, catalog no. 114.13D) as described in the manufacturer's protocols. Cells were plated in HITES medium (prepared in Ham's F12 plus 15 mM HEPES plus 0.8 mM $CaCl_2$) with 10% FCS on thin Matrigel (1:5 dilution). Serum was added for 24–48 hours to facilitate adherence and was then removed to minimize overgrowth of any remaining fibroblasts. Isolated primary alveolar epithelial cells from animals were plated in HITES media (prepared in Ham's F12 plus 15 mM HEPES plus 0.8 mM $CaCl_2$) plus 10% FCS on thin Matrigel (1:5 dilution) in the presence or absence of Brefeldin A (10 mg/ml; Sigma-Aldrich) for 4 hours. At the end of the culture period, media were collected, and cells scraped into lysis buffer for immunoblotting.

Depletion of the microbiota. WT and $Cxcr2^{-/-}$ mice were treated with or without antibiotic-containing water (ampicillin 0.5 mg/ml, neomycin 0.5 mg/ml [Pharmacia], gentamycin 0.5 mg/ml [Sigma-Aldrich], vancomycin 0.5 mg/ml [Sigma-Aldrich], and metronidazole 0.5 mg/ml [Sigma-Aldrich]) for 7 days, in a protocol modified from a previously published report (40). In addition, the water was supplemented with 1.5 mg/ml sucralose so as to improve taste and fluid intake.

Cxcl5 expression in the ileum. The BM-reconstituted mice were perfused with 20 ml saline from the left ventricle of the heart to clear the blood cells from the gut. The terminal ileum samples were collected and flushed with saline to eliminate luminal contents, then weighed and homogenized into 1.4 ml saline. After centrifugation, the supernatants were measured for Cxcl5 expression using ELISA.

Immunofluorescence analysis for Cxcl5 in the lung and ileum. WT and $Cxcl5^{-/-}$ mice were intravenously injected with 0.25 mg brefeldin A in 0.5 ml PBS (41). After 6 hours, the mice were sacrificed and perfused with saline from both the right and left ventricles of the heart. The lung and terminal ileum samples were collected and fixed in formalin overnight, then processed and embedded in paraffin. The specimens were cut in 4-μm sections, then the sections were deparaffinized by rinsing twice with xylene for 5 minutes each time, rehydrated in a series of alcohol, washed in PBS, and subjected to antigen retrieval in Tris-HCl buffer, pH 9.0, at 100°C in a water bath for 20 minutes. The slides were left to cool in the buffer for 20–30 minutes and incubated for 10 minutes with 3% H_2O_2 to block endogenous peroxidase, then the sections were sequentially stained with rabbit anti-mouse Cxcl5 antibody (Peprotech Inc.), DyLight 488–conjugated goat anti-rabbit IgG (Jackson ImmunoResearch), mouse anti-ABCA3 mAb (Abcam), Alexa Fluor 594–conjugated donkey anti-mouse IgG (Invitrogen), and DAPI, followed by air drying and mounting in polyvinyl alcohol. Slides were washed in PBS between incubations and dipped in distilled H_2O before drying.

16S rDNA sample acquisition and quantification of 16S rDNA. Cecal contents were collected and total DNA extracted using the QIAamp DNA Stool Mini Kit (stool pellet/luminal samples; Qiagen Inc.) or the DNeasy Blood and Tissue Kit (tissue samples; Qiagen Inc.). Quantification of 16S rDNA was performed by real-time RT-PCR using degenerate bacterial 16S rDNA specific primers (5′-AGAGTTTGATCCTGGCTCAG-3′; forward), (5′-CTGCT-GCCTYCCGTA-3′; reverse), (5′-FAM-TA+ACA+CATG+CA+AGTC+GA-BHQ1-3′; probe; + precedes the position of LNA base) (28).

16S rDNA sequencing and data analysis. 16S rDNA amplicons were sequenced as described previously (42), but the PCR was carried out for 30 cycles to guarantee amplification using the DNA obtained from the antibiotic-treated samples. Amplicons were sequenced using a 454 Genome Sequencer Junior. Sequences were decoded and processed using the QIIME software package and custom R package code (43). After decoding and quality control, a total of 58,968 sequences were used to build Operational Taxonomic Units (OTUs) at 97% sequence similarity, and only OTUs with at least 5 overall sequences were used in the remainder of the analysis. The data were analyzed using unweighted and weighted Unifrac. Observed differences in Unifrac distances between antibiotic treated groups, within and between genotypes, as well as differences in Unifrac distances between control mice of both genotypes, were tested for significance using a t test, and the reported P values were corrected for multiple comparisons using a Monte Carlo permutation procedure with 10,000 iterations.

Statistics. We performed all other statistical analyses with the GraphPad Prism software (version 4). Data are presented as means ± SEM, and a P value less than 0.05 was considered significant. We used a 2-way ANOVA or 2-tailed Student's t test as appropriate to compare data sets.

Study approval. All experiments with mice were conducted in accordance with the Institutional Animal Care and Use Committee of the Children's Hospital of Philadelphia.

Address correspondence to: Junjie Mei, Children's Hospital of Philadelphia, Division of Neonatology, 3516 Civic Center Blvd., ARC #414E, Philadelphia, Pennsylvania 19104, USA. Phone: 267.426.7228; Fax: 215.590.4267; E-mail: meij@email.chop.edu. Or to: G. Scott Worthen, Children's Hospital of Philadelphia, Division of Neonatology, 3516 Civic Center Blvd., ARC #416H, Philadelphia, Pennsylvania 19104, USA. Phone: 267.426.0198; Fax: 215.590.4267; E-mail: worthen@email.chop.edu.

1. Witko-Sarsat V, Rieu P, Descamps-Latscha B, Lesavre P, Halbwachs-Mecarelli L. Neutrophils: molecules, functions and pathophysiological aspects. *Lab Invest*. 2000;80(5):617–653.

2. Pillay J, et al. In vivo labeling with 2H2O reveals a human neutrophil lifespan of 5.4 days. *Blood*. 2010; 116(4):625–627.

3. Christopher MJ, Link DC. Regulation of neutrophil homeostasis. *Curr Opin Hematol*. 2007;14(1):3–8.

4. Eash KJ, Greenbaum AM, Gopalan PK, Link DC. CXCR2 and CXCR4 antagonistically regulate neutrophil trafficking from murine bone marrow. *J Clin Invest*. 2010;120(7):2423–2431.

5. Suratt BT, et al. Role of the CXCR4/SDF-1 chemokine axis in circulating neutrophil homeostasis. *Blood*. 2004;104(2):565–571.

6. Richards MK, Liu F, Iwasaki H, Akashi K, Link DC. Pivotal role of granulocyte colony-stimulating factor in the development of progenitors in the common myeloid pathway. *Blood*. 2003;102(10):3562–3568.

7. Lord BI, et al. The kinetics of human granulopoiesis following treatment with granulocyte colony-stimulating factor in vivo. *Proc Natl Acad Sci U S A*. 1989;86(23):9499–9503.

8. Semerad CL, Liu F, Gregory AD, Stumpf K, Link DC. G-CSF is an essential regulator of neutrophil trafficking from the bone marrow to the blood. *Immunity*. 2002;17(4):413–423.

9. Kim HK, De La Luz Sierra M, Williams CK, Gulino AV, Tosato G. G-CSF down-regulation of CXCR4 expression identified as a mechanism for mobilization of myeloid cells. *Blood*. 2006; 108(3):812–820.

10. Semerad CL, et al. G-CSF potently inhibits osteoblast activity and CXCL12 mRNA expression in the bone marrow. *Blood*. 2005;106(9):3020–3027.

11. Petit I, et al. G-CSF induces stem cell mobilization by decreasing bone marrow SDF-1 and up-regulating CXCR4. *Nat Immunol*. 2002;3(7):687–694.

12. Burdon PC, Martin C, Rankin SM. The CXC chemokine MIP-2 stimulates neutrophil mobilization from the rat bone marrow in a CD49d-dependent manner. *Blood*. 2005;105(6):2543–2548.

13. Stark MA, Huo Y, Burcin TL, Morris MA, Olson TS, Ley K. Phagocytosis of apoptotic neutrophils regulates granulopoiesis via IL-23 and IL-17. *Immunity*. 2005;22(3):285–294.

14. Buonocore S, et al. Innate lymphoid cells drive interleukin-23-dependent innate intestinal pathology. *Nature*. 2010;464(7293):1371–1375.

15. Cua DJ, Tato CM. Innate IL-17-producing cells: the sentinels of the immune system. *Nat Rev Immunol*. 2010;10(7):479–489.

16. Yu JJ, Gaffen SL. Interleukin-17: a novel inflammatory cytokine that bridges innate and adaptive immunity. *Front Biosci*. 2008;13:170–177.

17. Kobayashi Y. Neutrophil infiltration and chemokines. *Crit Rev Immunol*. 2006;26(4):307–316.

18. Stillie R, Farooq SM, Gordon JR, Stadnyk AW. The functional significance behind expressing two IL-8 receptor types on PMN. *J Leukoc Biol*. 2009; 86(3):529–543.

19. Tsai WC, Strieter RM, Mehrad B, Newstead MW, Zeng X, Standiford TJ. CXC chemokine receptor CXCR2 is essential for protective innate host response in murine Pseudomonas aeruginosa pneumonia. *Infect Immun*. 2000;68(7):4289–4296.

20. Tateda K, et al. Chemokine-dependent neutrophil recruitment in a murine model of Legionella pneumonia: potential role of neutrophils as immunoregulatory cells. *Infect Immun*. 2001;69(4):2017–2024.

21. Mei J, et al. CXCL5 regulates chemokine scavenging and pulmonary host defense to bacterial infection. *Immunity*. 2010;33(1):106–117.

22. Cacalano G, et al. Neutrophil and B cell expansion in mice that lack the murine IL-8 receptor homolog. *Science*. 1994;265(5172):682–684.

23. Shuster DE, Kehrli ME Jr, Ackermann MR. Neutrophilia in mice that lack the murine IL-8 receptor homolog. *Science*. 1995;269(5230):1590–1591.

24. Doisne JM, et al. Cutting edge: crucial role of IL-1 and IL-23 in the innate IL-17 response of peripheral lymph node NK1.1- invariant NKT cells to bacteria. *J Immunol*. 2011;186(2):662–666.

25. Chung Y, et al. Critical regulation of early Th17 cell differentiation by interleukin-1 signaling. *Immunity*. 2009;30(4):576–587.

26. Sutton CE, Lalor SJ, Sweeney CM, Brereton CF, Lavelle EC, Mills KH. Interleukin-1 and IL-23 induce innate IL-17 production from gammadelta T cells, amplifying Th17 responses and autoimmunity. *Immunity*. 2009;31(2):331–341.

27. Liu Y, et al. IL-17A and TNF-alpha exert synergistic effects on expression of CXCL5 by alveolar type II cells in vivo and in vitro. *J Immunol*. 2011; 186(5):3197–3205.

28. Hill DA, et al. Metagenomic analyses reveal antibiotic-induced temporal and spatial alterations in intestinal microbiota with associated alterations in immune cell homeostasis. *Mucosal Immunol*. 2010; 3(2):148–158.

29. Furze RC, Rankin SM. Neutrophil mobilization and clearance in the bone marrow. *Immunology*. 2008; 125(3):281–288.

30. Kwon JH, Keates AC, Anton PM, Botero M, Goldsmith JD, Kelly CP. Topical antisense oligonucleotide therapy against LIX, an enterocyte-expressed CXC chemokine, reduces murine colitis. *Am J Physiol Gastrointest Liver Physiol*. 2005; 289(6):G1075–G1083.

31. Round JL, Mazmanian SK. The gut microbiota shapes intestinal immune responses during health and disease. *Nat Rev Immunol*. 2009;9(5):313–323.

32. Gaboriau-Routhiau V, et al. The key role of segmented filamentous bacteria in the coordinated maturation of gut helper T cell responses. *Immunity*. 2009;31(4):677–689.

33. Ivanov II, et al. Induction of intestinal Th17 cells by segmented filamentous bacteria. *Cell*. 2009; 139(3):485–498.

34. Jeyaseelan S, et al. Induction of CXCL5 during inflammation in the rodent lung involves activation of alveolar epithelium. *Am J Respir Cell Mol Biol*. 2005; 32(6):531–539.

35. Rossi DL, et al. Lungkine, a novel CXC chemokine, specifically expressed by lung bronchoepithelial cells. *J Immunol*. 1999;162(9):5490–5497.

36. Kohler A, et al. G-CSF-mediated thrombopoietin release triggers neutrophil motility and mobilization from bone marrow via induction of Cxcr2 ligands. *Blood*. 2011;117(16):4349–4357.

37. Kimura A, Kishimoto T. Th17 cells in inflammation. *Int Immunopharmacol*. 2011;11(3):319–322.

38. Khader SA, Gaffen SL, Kolls JK. Th17 cells at the crossroads of innate and adaptive immunity against infectious diseases at the mucosa. *Mucosal Immunol*. 2009;2(5):403–411.

39. Rivera-Nieves J, et al. L-selectin, alpha 4 beta 1, and alpha 4 beta 7 integrins participate in CD4+ T cell recruitment to chronically inflamed small intestine. *J Immunol*. 2005;174(4):2343–2352.

40. Rakoff-Nahoum S, Paglino J, Eslami-Varzaneh F, Edberg S, Medzhitov R. Recognition of commensal microflora by toll-like receptors is required for intestinal homeostasis. *Cell*. 2004;118(2):229–241.

41. Foster B, Prussin C, Liu F, Whitmire JK, Whitton JL. Detection of intracellular cytokines by flow cytometry. In: Coligan JE, et al., eds. *Current protocols in immunology*. 2007;Chapter 6:Unit 6.24.

42. Wu GD, et al. Sampling and pyrosequencing methods for characterizing bacterial communities in the human gut using 16S sequence tags. *BMC Microbiol*. 2010;10:206.

43. Caporaso JG, et al. QIIME allows analysis of high-throughput community sequencing data. *Nat Methods*. 2010;7:335–336.